AN INNOVATIVE PROTOTYPE OF AN AUTOMATIC DEVICE FOR MOVING fINGERS AND WRIST DURING FMRI ANALYSIS

ISSN 1590-8844
International Journal of Mechanics and Control, Vol. 26, No. 01, 2025
https://doi.org/10.69076/jomac.2025.0009

AN INNOVATIVE PROTOTYPE OF AN AUTOMATIC DEVICE FOR MOVING FINGERS AND WRIST DURING fMRI ANALYSIS

Gabriella Eula*

* Department of Mechanical and Aerospace Engineering, Politecnico di Torino, Torino, Italy

ABSTRACT

The paper presents an innovative active device capable of moving the fingers and the wrist of the human hand during fMRI (functional Magnetic Resonance Imaging). The prototype can be used both for motor learning studies and for stroke analysis. Various possible configurations were investigated. The first was an active glove. The second was a box in which the subject's hand is inserted, and then moved by pneumatic actuators. The authors optimized this configuration, and also developed an interesting design procedure using data from the literature, experimental measurements, numerical simulations, and experimental videos. This configuration moves the wrist in addition to the fingers, a feature which is innovative, useful and commonly found in devices of this kind.

Keywords: automatic devices for fMRI analysis; automatic machine to move hand during fMRI analysis; automatic system moving fingers during fMRI analysis

1 INTRODUCTION

fMRI (functional Magnetic Resonance Imaging) is a biomedical technique that provides information on the brain activities involved in a particular cognitive process or motor action by exploiting the effect of an external magnetic field. To avoid altering the quality of the brain image and harming the patient, it is essential that only non-magnetic materials be present in the MRI chamber. Selecting an appropriate actuation system type and materials is thus crucial. This imaging technique is employed to evaluate how the brain metabolism reacts after performing an action such as speaking, moving a limb, reading or thinking. The first scientists who studied this technique [1,2] understood the importance of evaluating blood oxygenation level in order to capture brain images. In general, when a human being performs a certain action, a part of the blood flow circulates within a certain brain area: in particular, for each action that a human performs, a different area of the brain is activated.

Contact author: Gabriella Eula[1]

[1]Corso Duca Degli Abruzzi 24, Torino, TO, 100129, Italy
E-mail: gabriella.eula@polito.it

This area is supplied with blood so that the action can be transported to the rest of the body via muscles and nerves. When blood flow increases, the level of oxygen present in it also increases proportionally: this variation is recorded by magnetic resonance imaging thanks to the change in magnetism of the hemoglobin present in the blood. The use of technology in rehabilitation is a therapeutic opportunity for patients who have suffered a serious accident or people born with particular disabilities. Over the last 15 years, the use of rehabilitation technology has become much more common, while the quality of the devices employed has also increased considerably. A number of studies have addressed finger movements and mechanisms acting on the fingers [3,4]. Many devices used to move the fingers during fMRI imaging feature a glove structure using various kinds of actuation [5-13], based in particular on inflatable silicone pneumatic actuators [10,13]. Some devices also provide wrist movement [8,14,15]. In some systems, the fingers are actuated by external silicon pneumatic actuators [10] on the upper side of each finger and secured in a textile structure.
Other devices use a mechanism on the upper side of each finger to guide the finger movement from this point [16, 17], or employ cable drives [8,11,12]. Some systems were also designed to measure finger grasping force [15,18-20], to provide a better understanding of hand movements [21-27] or to be used both for rehabilitation purposes and for fMRI analysis [5-7, 22, 28-43]. Actuation is often pneumatic, as in the cases where inflatable actuators are

used [10,13]. In an application designed for use in the patient's home without supervision by a physiotherapist [35], the hand is inserted in a box where physiological finger positions are replicated and forces can be imposed to perform rehabilitation exercises for flexion and extension movements of the metacarpophalangeal joint (MP joint) and the proximal interphalangeal joint (PIP joint) of the index, middle, ring and little fingers. However, they are not specific applications for fMRI analysis. In a study conducted on primates [27] in which fingers were immobilized using a soft cast, a restriction "of the cortical areas corresponding to the distal part of the upper limb and an expansion of the most proximal areas of the arm that maintain active contact with the environment" was observed. This study found that when the fingers were immobilized their function decreased, but wrist and forearm function increased. These effects were reversed when the soft casts immobilizing the fingers were removed. The glove prototype presented in [5] was worn by a healthy human subject lying supine on the fMRI analysis table. During this test, the MRC-Glove was activated five times in 30-second blocks. During fMRI analysis carried out while moving the fingers of the human hand, a possible cycle time can be 3s for finger flexion and 3s for finger extension. This procedure is performed for a continuous period of 30s followed by a 21s rest [6]. This study was carried out at a supply pressure of 2 bar, analyzing the movements of all fingers except the thumb. Wrist movements were not analyzed. The pneumatic actuators whereby finger joints can be bent were operated non-simultaneously. In previous work, the present authors designed and constructed a prototype to move a subject's foot or feet during fMRI analysis [43,44]. The results obtained were good and demonstrated the prototype's reliability.

This article presents a study useful for the design of an innovative active device able to work in a magnetic resonance chamber during fMRI analysis, moving the subject's finger/fingers or his wrist according to physiological and non-physiological trajectories, so that the brain areas activated during this movement can be studied. The information thus obtained can be used to identify possible ways of recovering hand motor functions in patients with brain injuries so that they can engage in daily activities that would otherwise be impossible. The wrist motion for these analyses, both on healthy people and on patients, has been considered by our clinicians useful for the purposes of the analysis itself and constitutes an originality of the machine compared to the most frequent layouts of them. The non-glove structure of the machine was also judged to be more versatile. It also allows not only the imposition of certain trajectories to the fingers, but also to impose non-physiological trajectories, useful for motor learning studies.This machine can be useful in general: for motor learning studies; for rehabilitation training settings especially related to brain recovery; for fMRI analysis useful for preliminary evaluations for neurological surgical interventions.

2 PRESENTATION OF THE PROTOTYPE

The device must be designed to ensure that, during tests in the magnetic resonance chamber, the hand performs passive movements, i.e., thanks to the application of an external force, without actively contracting the muscles. Specifically, the subject's left hand must perform the following movements: complete flexion and extension of each finger individually while keeping the remaining fingers extended; complete and simultaneous flexion and extension of the index, middle, ring and little fingers; complete flexion and extension of the wrist. The term flexion refers to that movement of the body that decreases the angle between the structures or joints involved, bringing them further together. Extension is the opposite movement, in which the angle increases and the structures or joints move away from each other. Flexion of the fingers thus consists of bending the phalanges towards the palm of the hand, while extension consists of straightening the fingers.

Wrist flexion occurs when the wrist is bent towards the palm of the hand, while wrist extension occurs when the wrist is bent upwards. Given the particular nature of the application environment, selecting appropriate materials is of fundamental importance to guarantee correct device operation and patient safety, as no ferromagnetic materials can be introduced in the magnetic resonance (MR) chamber. The first stage of this study consisted of designing gloves where the fingers and the wrist were moved using silicon pneumatic actuators constructed in the laboratory.

Details of the first glove protype with silicon pneumatic actuators located atop each finger are shown in Figure 1.

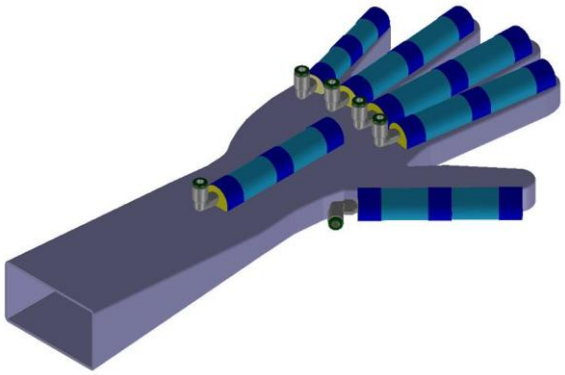

Figure 1 First prototype of an active glove controlled by means of silicon pneumatic actuators.

With this design, the correct physiological trajectory of the fingers cannot be readily controlled and monitored because of the deformability of the textile structure. In addition, the stiffness and the deformation of each silicon actuator make it difficult to determine whether or not the finger is moved through the natural physiological trajectory. However, this information is important in enabling the clinicians who move the fingers during fMRI analysis to understand brain function. Consequently, the design shown in Figure 2a was developed. In this case, the person places their hand in a box and the fingers are moved using standard external

ISSN 1590-8844
International Journal of Mechanics and Control, Vol. 26, No. 01, 2025
https://doi.org/10.69076/jomac.2025.0009

linear pneumatic cylinders. In this configuration, however, interference can occur between the moving cylinder and the finger, as shown in Figures 2b and c. Moreover, the finger's trajectory can differ from the physiological path and is difficult to check. In addition, this design features an actuator for each finger, thus increasing the number of components, costs, control system complexity, weight, and device bulk. Lastly, the authors developed the design illustrated in Figures 3a and 3b, which is the prototype presented here. This prototype can also move the wrist, as established in the beginning of this study. This can be useful for further studies of brain function. The prototype features a single linear actuator for all fingers, a pneumatic motor for the thumb, and a linear actuator for the wrist.
The design of this final prototype started from the analysis of each finger's movement during passive exercises performed with the assistance of a physiotherapist, a situation in which finger trajectories are well controlled.

Figure 2a The first prototype with a box geometry, showing the hand inside.

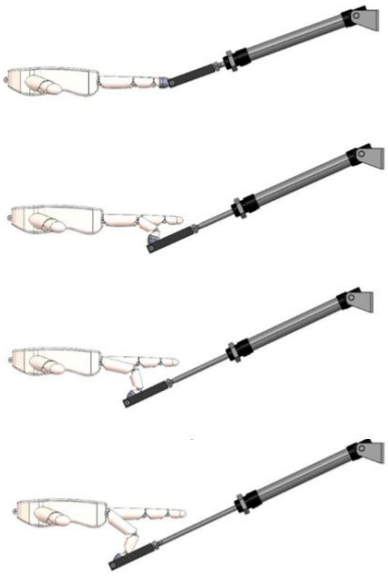

Figure 2b Finger movement in the first box prototype.

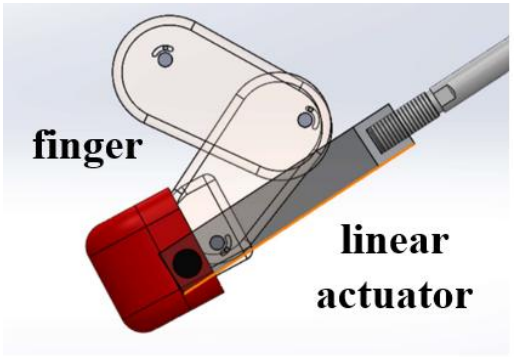

Figure 2c A detail of possible interference between the pneumatic cylinder and the finger.

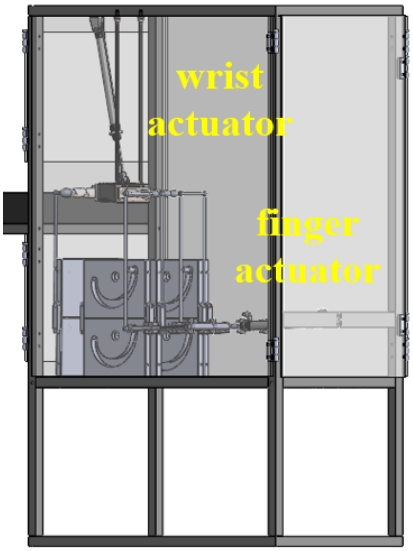

Figure 3a The final prototype structure.

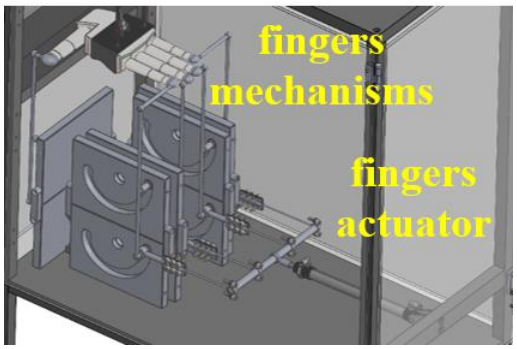

Figure 3b Detail of the single linear pneumatic actuator for all fingers.

The automatic machine must be capable of reproducing these trajectories, which are important for brain activation study during fMRI analysis. Various kinds of brain activation during finger movement can be investigated by using physiological and non-physiological fingers and wrist trajectories. This final layout connects each finger to a vertical link (Figures 4a) which is in turn connected to a non-driven pin moving in a crescent-shaped slot and mounted on a telescopic shaft (Figure 4b). The slot can reproduce a physiological trajectory or a non-physiological

trajectory in order to move the finger along a known path and investigate the resulting brain activation. The prototype foresees to use the compressed air as kind of actuation, as it is compatible with the RM chamber, safe, clean and easy to use in hospitals too. In particular this machine allows to move all fingers together or one or more than one, with the patient in a passive state. The Figure 4a shows the mechanisms for all the fingers and also for the thumb.
The Figure 4b shows some details of the system designed to move the subject's fingers. A non-driven pin is inserted in the slot and connected to a telescopic shaft rotating along a horizontal axis and each finger is connected to a link put between the finger and the non-driven pin. The subject's fingertips are inserted in thimbles on each link. Activating the telescopic shaft rotation, it is possible to move the link, and so the finger to it connected, and to obtain the required finger movement for the brain functioning study. Trajectories can be obtained experimentally by analyzing videos, and numerically from measurements of each finger's phalanges, as then here explained. They can be then compared with other trajectories from the applicable literature. They allow to design properly the slot. So this design is capable of moving each finger (or all fingers together) along known, accurate trajectories established by the clinicians and the trajectories may be physiological or non-physiological. In Figure 4c the movement C (then described in detail) is shown, as an example of movement to design the slot. Analysing the physiological trajectory of each finger in a healthy subject, the slot shown in Figure 4b can be designed.

2.1 FINGER MOVEMENT

The physiological Range of Movement (ROM) for the finger phalanges and wrist are: proximal phalanx 0°-90°; middle phalanx 0°-110°; distal phalanx 0°-90°; wrist 0°-85° [25,27]. Following the literature [39], finger trajectories are analyzed in plane [x,y], where x is directed along the finger and y is perpendicular to x, as shown in Figure 5.

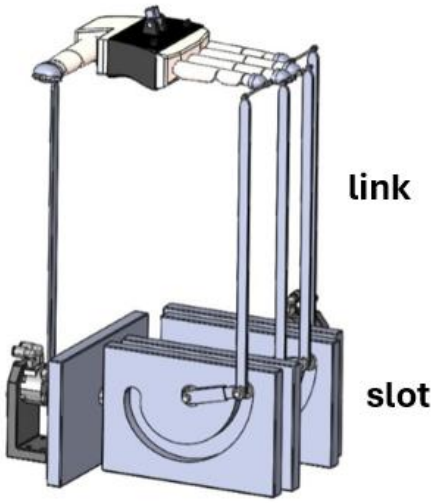

Figure 4a The mechanisms designed to move all the fingers and the thumb.

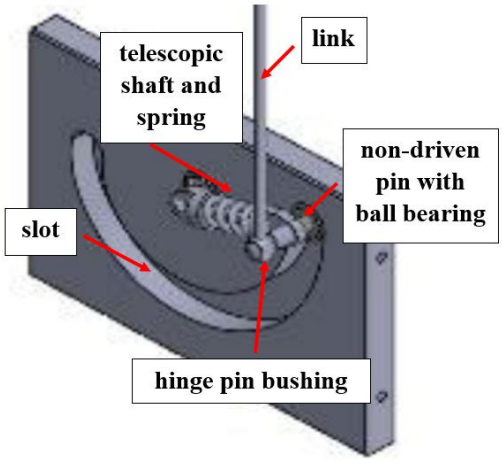

Figure 4b A detail of the slot and of the part of mechanism used to guide the finger.

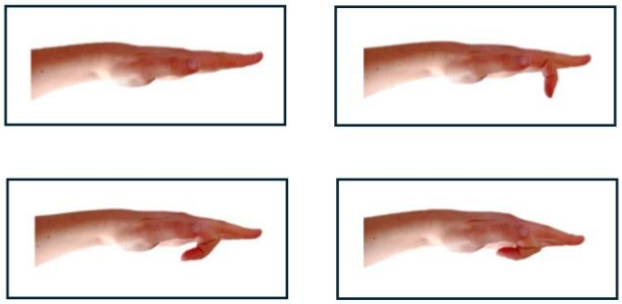

Figure 4c The movement (here C) imposed on the fingers.

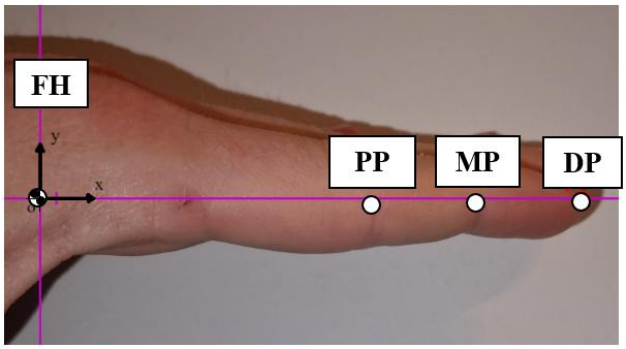

Figure 5 The reference system adopted for the index finger.

Figure 5 shows the phalanges and the reference system adopted for this study. FH is the base of the proximal phalanx, here considered fixed, PP is the head of the proximal phalanx, MP is the base of the middle phalanx, and DP is the head of the distal phalanx. In particular, three possible movements designated as A, B, C were investigated. Figure 6a shows the angles used for the phalanges trajectories [21], while Figures 6b, c, d illustrate the angles α, β, γ in each movement (A, B, C) considered and then used to model the finger movement in a calculation software. The angles α, β, γ are the main angles used to model finger movement with calculation software program. In movement A, only the distal and middle phalanges of the index finger are moved, and the proximal phalanx is kept stationary.

ISSN 1590-8844
International Journal of Mechanics and Control, Vol. 26, No. 01, 2025
https://doi.org/10.69076/jomac.2025.0009

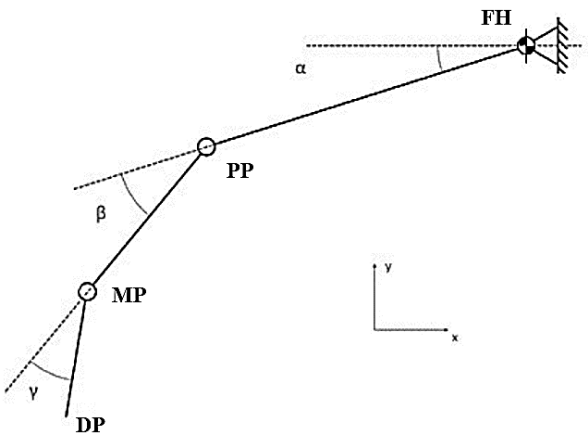

Figure 6a The angles involed in the study of the phalanges trajetories.

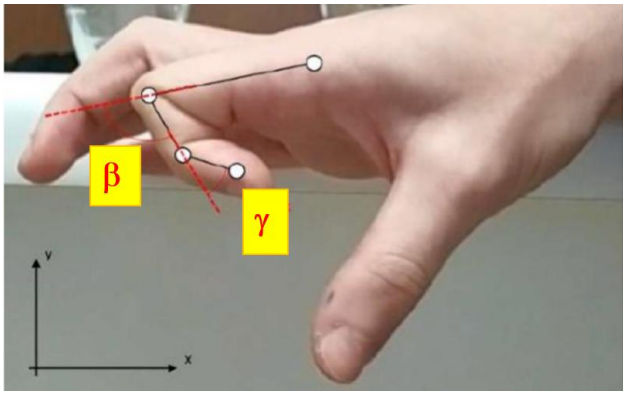

Figure 6b Details of movement A.

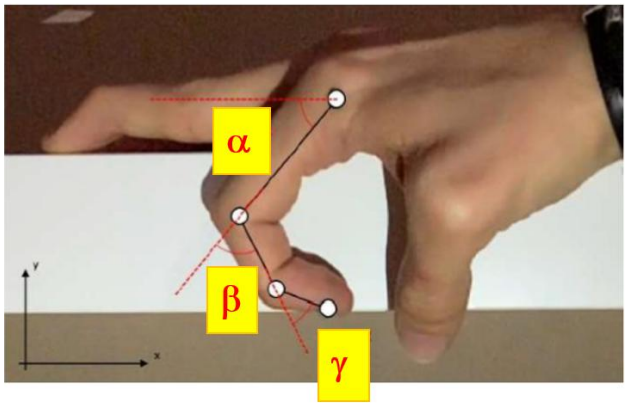

Figure 6c Details of movement B.

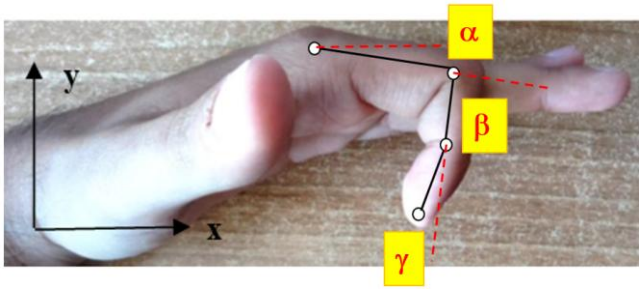

Figure 6d Details of movement C.

In movement B, all phalanges of the index finger are moved, while all other fingers are stationary, extended and resting on a rigid fixed support. In movement C, all the phalanges of the index finger are moved, while the other fingers are extended but not supported. As movement C yields the most physiological trajetories, it was selected for the subsequent studies and design stages.

2.2 WRIST MOVEMENT

In agreement with several clinicians, the authors decided to move the subject's wrist with this device. This can also be useful for fMRI analysis. Figure 7a shows the movement to be imposed on the subject's hand. Figure 7b shows the linear pneumatic actuator connected to the subject's hand in order to move it as shown in Figure 7a.

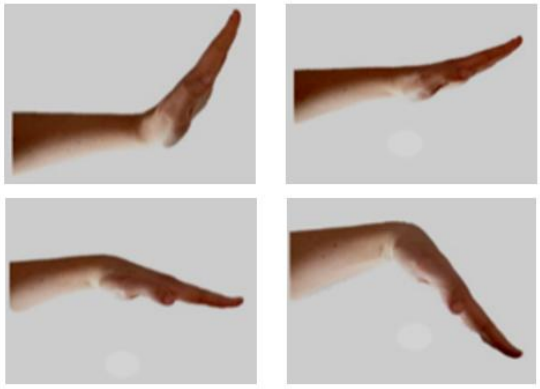

Figure 7a Details of the movement imposed on the wrist.

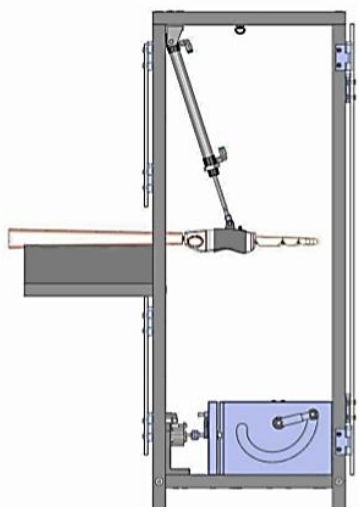

Figure 7b The linear pneumatic actuator to move the wrist.

3 STUDY FLOWCHART

The steps of the design process presented here realised are illustrated in Figure 8. The process involves: producing videos of finger movements, which are then analyzed using specific software to establish the experimental finger trajectories; reviewing the trajectories presented in the literature; carrying out experimental measurements on multiple subjects, determining the length of each phalanx of each finger and then calculating the finger trajectories for

the average male hand and the average female hand; comparing the trajectories presented in the literature (with similar subjects), the trajectories calculated from phalange measurements, and the trajectories from the experimental videos; transferring this information to CAD software in order to construct slots for the average male and average female hands.

4 FINGER MEASUREMENTS USED FOR SLOT DESIGN

The most important parts of this device are the slots that establish the movement of the fingers. Multiple measurements were taken of both hands of several subjects and using different kinds of caliper, in order to design slots for average male and female subjects. The number of subjects examined can already be considered useful for the design analyses for which it is intended.

In this paper the tests carried out analysing the index finger were illustrated, but the method can be applied also to the other fingers. Furthermore, for brevity sake, only some of the all measurements carried out on men and women are here presented, illustrating only male subjects. In all the tables presented, SD means Standard Deviation. The data collected by operator 1 for the right hands of 10 healthy right-handed subjects are shown in Table 1. Measurements were made with a digital caliper with the hand extended on a flat surface. Table II shows the data collected by operator 2 on 20 subjects. Measurements were made using standard caliper on the left hand extended on a flat surface. Table III shows data referring to movement C collected on two subjects by operator 3 using a standard caliper with the right hand on a flat surface. Figure 9 shows the index finger trajectory calculated by operator 2 for the left hand of a 23 year old male subject, body mass 60 kg, height 1.77 m, proximal phalanx 45 mm, medium phalanx 27 mm, distal phalanx 15 mm (also illustrated in Table I), using the reference system illustrated in Figure 5, with the same finger initial position. Measurements were taken by several different operators. For the sake of brevity, Tables I, II and III show only some of the measurements. The different operators' measurements can be readily compared by looking at the index finger dimensions: operator 1, right hand, subject height 1.78 m, digital caliper, index finger length 96.9 mm; operator 2 left hand, subject height 1.78 mm, standard caliper, index finger length 82.7 mm; operator 3, right hand, subject height 1.78 m, standard caliper, index finger length 84.5 mm; operator 1, left hand, subject height 1.82 m, digital caliper, index finger length 93.1 mm. The differences in these measurements stem from the use of both digital and standard calipers: the digital caliper gives better measurement results. In addition, the experimental results obtained from these measurements were analyzed by means of different techniques proposed in the literature: statistical parameters (average value, standard deviation); correlation between hand dimensions and subject height [45-50] considering the proportionality of these values and using different methods (Pearson linear correlation coefficient [51] with the Anderson-Darling test [52] and the Shapiro-Wilk test [53]); linear regression with the t-Student test [54]; the ratio between the length of the phalanges (average differences) [55,56]).

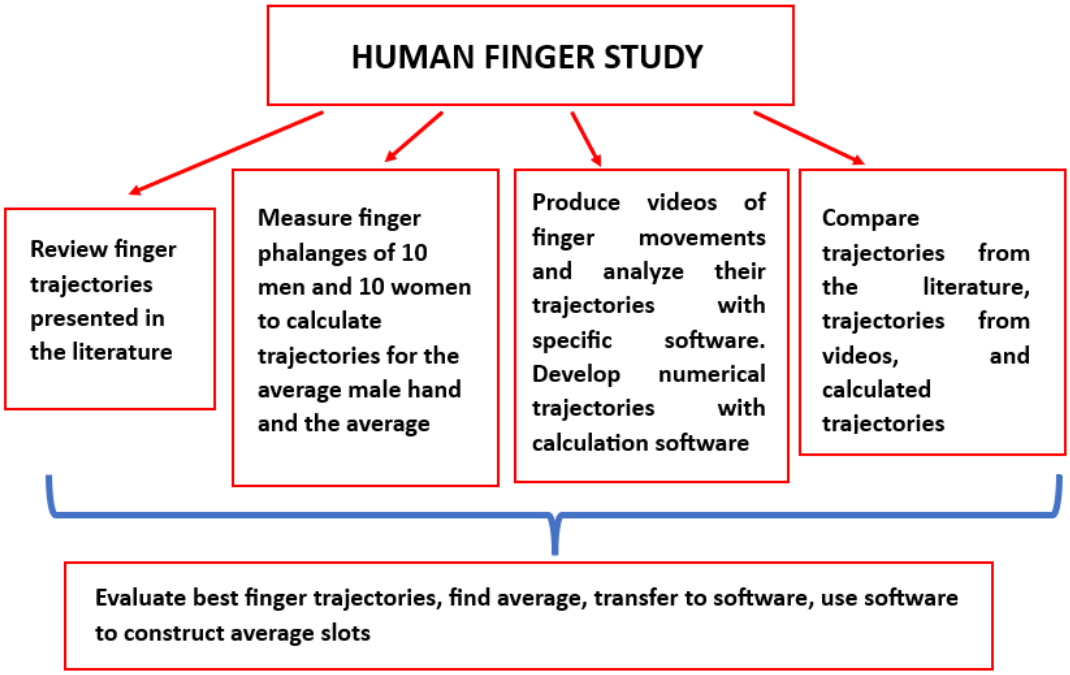

Figure 8 Steps of the slot design process.

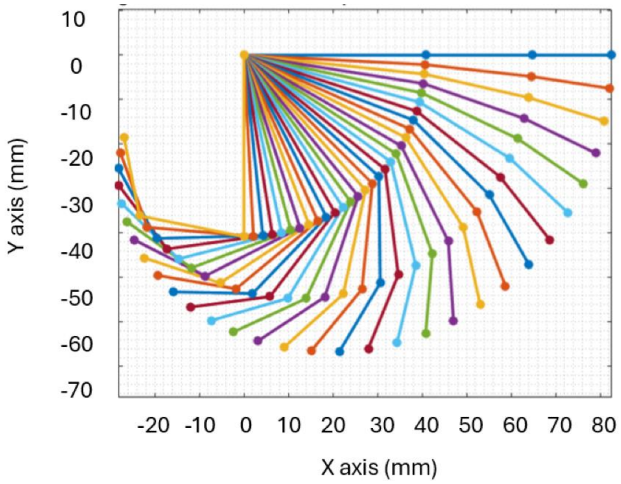

Figure 9 Preliminary example of a calculated trajectory of the index finger phalanges.

It should be noted that there are non-negligible differences of up to 11% between some of these calculations. These differences may be due to various factors. First, the study does not distinguish between sex and gender: values are calculated for both sexes and some studies cited earlier [48] highlight a difference in length relationships. Furthermore, an error may arise from the fact that the measurements were taken from the back of the finger in the joint halfway up the height of the finger (the free end), thus with a certain angle that increases the dimension. To obtain additional information, Student's t-test [54] was carried out (after passing the appropriate controls) on the values of ratios other than 1 (with $\alpha = 0.05$); p-values were 0.88 for the female gender and 0.77 for the male gender. The p-value is the probability that the results from the sample data occurred by chance; α is the threshold of statistical significance established by the operator, and represents the probability of type I error. On the basis of these considerations, average male hand and female hand dimensions were calculated and used to design the corresponding slots. By way of example, Table IV shows the characteristics of average male and female right hands from operator 1 measurements. The average fingers were obtained using operator 1 measurements as he used the digital caliper. In particular, phalange measurements were used to construct the index finger trajectory in the [x, y] plane using calculation software, to analyze the index finger trajectory obtained from experimental videos, and to construct the index finger geometry in a specific software program. All these results were then compared with each other and with similar trajectories obtained from the literature. Figure 10 shows experimental and numerical trajectories obtained by the authors with the subjects indicated in Table I from which average valves were calculated. Here h is the height of the subject. The trajectory shown in black in Figure 10 is from the literature [39,49] and it is the index finger trajectory with proximal phalanx 43 mm, medial phalanx 28 mm, distal phalanx 25 mm. The results obtained are good and demonstrate the study's reliability. The authors will carry out further experimental analyses using specific software to analyze finger movements and determine the corresponding trajectory. This is also important in developing a method for analyzing these movements precisely and to carry out accurately all these studies.

5 FINGER TRAJECTORIES

The procedures described above can be employed to design a slot for use by average adult male and female subjects. The slots are machined in interchangeable plates that can be installed on the device to reproduce different physiological and non-physiological trajectories. For the clinicians it is important to know the real trajectory imposed in order to analyse it together with the corresponding brain activation. The position of the links can be maintained exactly vertical or not, on the basis of the required finger movement.

Table I - Subjects examined by operator 1: right index finger

Subject	Age	Body mass (kg)	Height (m)	Proximal phalanx (mm)	Middle phalanx (mm)	Distal phalanx (mm)	Total length (mm)
M1	30	82.7	180.0	45.41	24.70	20.22	90.3
M2	26	64.0	174.7	44.75	24.29	24.09	93.1
M3	27	72.1	191.5	48.53	30.55	26.65	107
M4	26	79.1	177.5	49.74	28.82	23.03	101.6
M5	26	60.5	172.5	39.33	23.24	21.44	84.0
M6	25	67.0	174.2	39.51	24.59	24.02	88.1
M7	33	65.4	174.9	51.44	27.50	24.53	103.5
M8	30	79.1	183.5	55.36	27.94	25.19	108.5
M9	30	69.7	177.6	45.74	28,.79	24.64	99.2
M10	30	59.2	179.9	47.41	23.67	23.64	94.7
SD				4.98	2.59	1.84	8.1
Averages	28.3	69.88	178.63	46.72	26.41	23.75	96.9

Table II - Subjects examined by operator 2: right index finger

Subject	Age	Body Mass (kg)	Height (m)	Proximal phalanx (mm)	Middle phalanx (mm)	Distal phalanx (mm)	Total length (mm)
M1	23	69	181.5	43	23	16	82
M2	28	67	169.0	39	23	17	79
M3	32	82	189.0	44	26	19	89
M4	41	73	171.0	40	24	18	82
M5	59	100	182.0	39	26	19	84
M6	29	60	167.0	36	20	20	76
M7	23	87	185.0	41	23	21	85
M8	26	71	175.0	38	23	21	82
M9	26	69	178.0	38	25	18	81
M10	31	96	188.0	44	24	17	85
M11	27	74	172.0	41	21	19	81
M12	54	76	179.0	44	27	17	88
M13	33	80	180.0	42	21	18	81
M14	61	91	177.0	42	24	18	84
M15	39	85	185.0	40	27	18	85
M16	25	59	161.0	39	21	16	.6
M17	24	86	182.0	41	26	17	84
M18	24	85	189.0	41	24	19	84
M19	23	60	177.0	45	27	15	87
M20	27	76	181.0	40	24	15	79
SD				2.37	2.14	1.71	3.5
Averages	32.75	77.30	178.43	40.85	23.95	17.9	82.7

Table III - Subjects examined by operator 3: right index finger

Subject	Age	Body Mass (kg)	Height (cm)	Proximal phalanx (mm)	Middle phalanx (mm)	Distal phalanx (mm)	Total length (cm)
M1	23	69	182	43	23	16	82
M2	23	60	177	45	27	15	87
SD				1.42	2.83	0.71	3.5
Averages	23	64.5	179.5	44.0	25.0	15.5	84.5

Table IV - Average male and female right hands from operator 1 measurements

Subject	Average phalanges (dimensions in mm)													
	Thumb		Index			Middle			Ring			Pinkie		
	FP	FD	FP	FM	FD	FP	FM	FD	FP	FM	FD	FP	FM	FD
Average male	43.56	34.01	53.01	33.59	26.20	58.33	40.31	27.80	54.50	38.34	27.30	43.76	29.00	24.60
Average female	39.56	29.32	49.14	30.75	22.50	53.24	36.01	24.50	49.40	33.83	24.40	41.32	24.70	21.90
SD male	4.34	2.35	3.57	2.47	2.19	3.25	3.07	1.96	2.42	3.17	1.92	2.84	2.49	1.90
SD female	2.29	3.04	3.67	1.98	1.25	4.29	2,30	1.62	3.59	2.28	1.69	2.31	1.99	1.66

ISSN 1590-8844
International Journal of Mechanics and Control, Vol. 26, No. 01, 2025
https://doi.org/10.69076/jomac.2025.0009

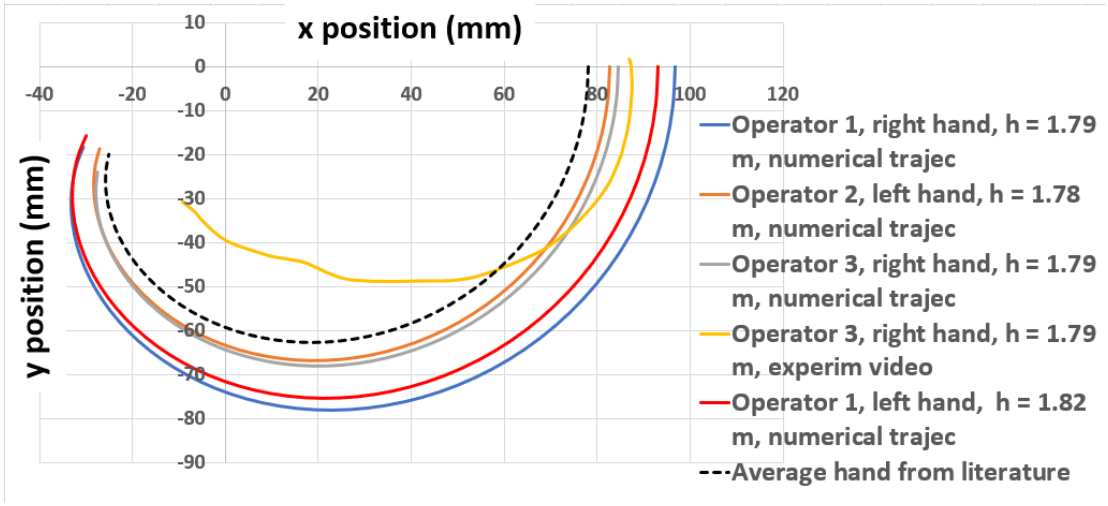

Figure 10 Index finger trajectories obtained in various conditions.

5.1 PHYSIOLOGICAL TRAJECTORIES

Many fMRI analyses, including those carried out for motor learning purposes, are performed while moving fingers along physiological paths. It is thus important to study and obtain these trajectories by means of a procedure such as that proposed above. Figure 11a shows the mechanism used to move the index finger along a physiological trajectory for an average male subject. The possibility of inclination of the link is very low, as the mechanism follows the finger trajectory in its same physiological cycle time and the condition of the subject has to be passive. A non verticality of the link means that the subject is not completely passive and this can be an important warning for the clinicians during the fMRI analysis. Anyway this possible inclination can be avoided as follows. The Figure 11b shows the mechanism where two identical slots are used together in order to maintain the link in a vertical position, if necessary. The non-circularity and the complexity of the slot shape favours the effect of this second slot also using a simple circular pin, fixed on the link. In this case it is important the choice of the materials in contact, in order to reduce the friction. The Figure 11c shows another solution where the possible inclination of the link is avoided using a cart type constraint, that also improves the sliding condition. However, the doctors' needs can be adequately met using the initial configuration with a single slot. Links can be connected to all fingers or to a single finger, thus moving all fingers simultaneously or one finger at a time. A reduction of the link length, compatible with the wrist movement, can also improve this aspect. This length reduction can be foreseen since the wrist movement can not be imposed together with the fingers motion. So the machine design can provide a horizontal flat bed to pull down the actuator and the fingers mechanisms when the wrist movement is activated. On the other hand, all these fingers mechanisms can be lifted up and positioned at an adequate distance for their motion, as shown in Figure 12.

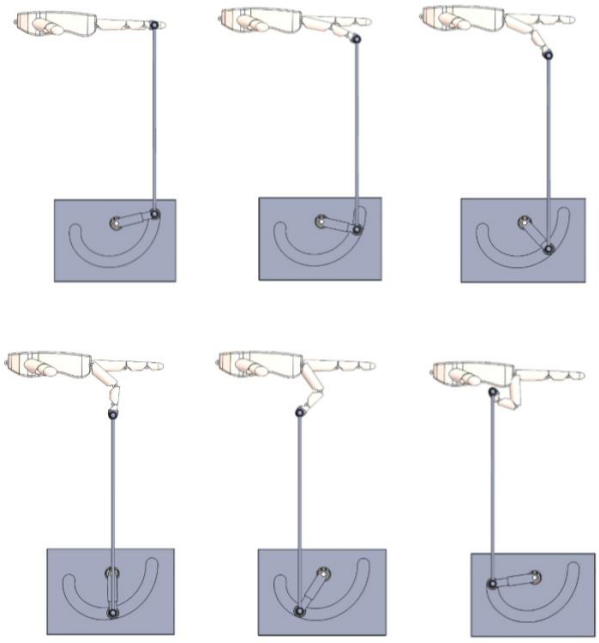

Figure 11a Finger movement along a physiological trajectory.

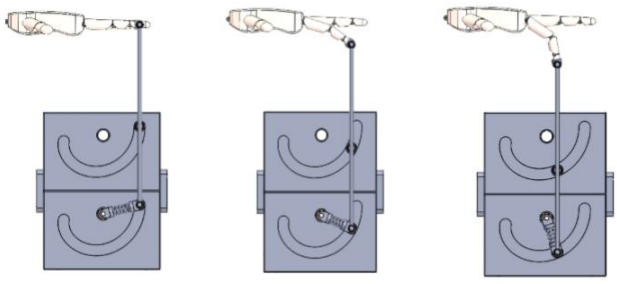

Figure11b Finger movement along a physiological trajectory (link maintained in the vertical position by using a second slot).

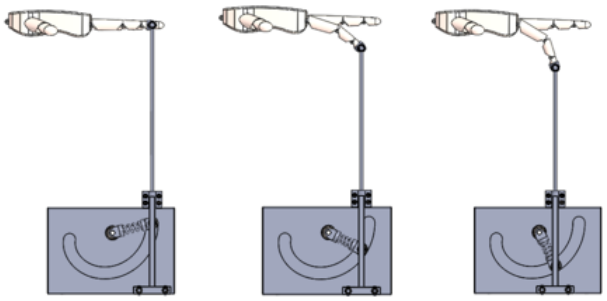

Figure11c Finger movement along a physiological trajectory (link maintained in the vertical position by using a cart type constraint).

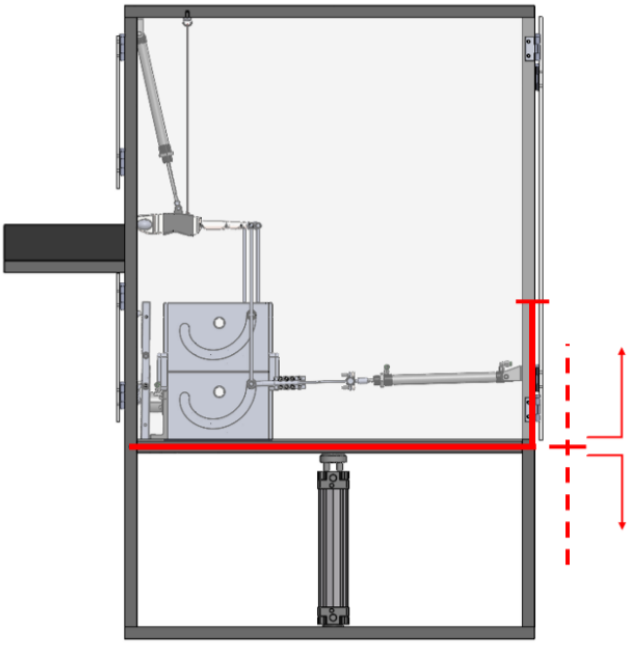

Figure 12 The possible system to move up and down vertically the platform with all the fingers mechanisms and actuators.

5.2 NON-PHYSIOLOGICAL TRAJECTORIES

The device's structure also makes it possible to move fingers and wrist along non-physiological paths. To this end, the trajectories are investigated experimentally and numerically in order to construct the corresponding slots. For clinicians, it is important to know the exact trajectory imposed by the device in order to analyse it together with the associated brain activation.

Depending on the type of movement required, links can be maintained in the vertical position or allowed to depart from it as the fingers are moved. Slots reproducing non-physiological trajectories can be designed after analyzing such movements experimentally and numerically. This can be useful for studies of brain function in healthy subjects and patients. Figure 13a shows the non-physiological movement considered here. The corresponding slot is shown in Figure 13b.

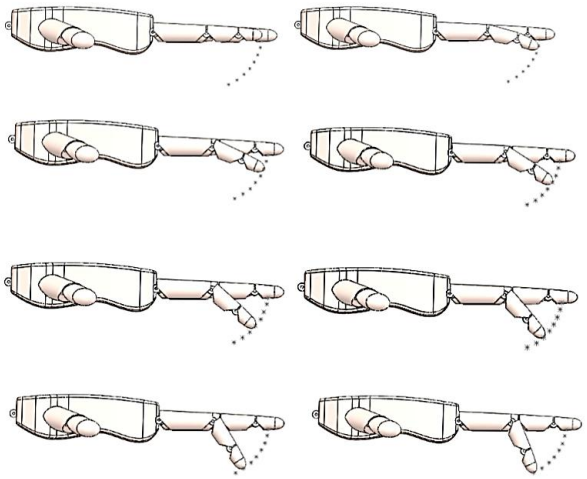

Figure 13a An example of a non-physiological finger trajectory.

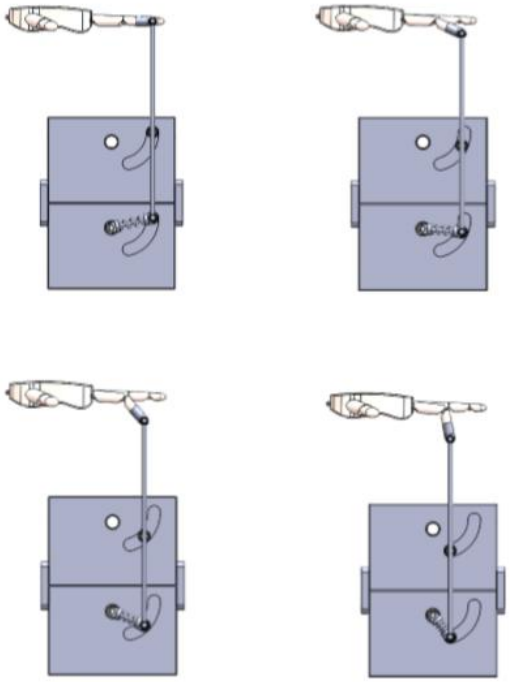

Figure 13b Non-physiological trajectory by clinicians.

6 SOME SOLUTIONS FOR FINGER MOVEMENT

Different kinds of drive or actuation can be used to move the telescopic shaft and hence the finger.

6.1 FIRST SOLUTION: BELT DRIVE

A belt drive can be connected to two fingers at the same time if necessary, as shown in Figure 14, where (1) are the pulleys and (2) are the belts. The same transmission structure is then used to move all the fingers. The pulleys are driven by pneumatic motors. Drawbacks of this configuration include its bulk, its large number of parts and motors, and the need to ensure correct belt tension at all times.

ISSN 1590-8844
International Journal of Mechanics and Control, Vol. 26, No. 01, 2025
https://doi.org/10.69076/jomac.2025.0009

6.2 SECOND SOLUTION: SINGLE PNEUMATIC ACTUATOR

In this configuration, a linear pneumatic actuator can be connected to one or all fingers. The mechanism is illustrated in Figure 15: the linear actuator, slots and vertical link are shown on the left, while the new geometry of the telescopic shaft is shown on the right. Here a spring is added to guarantee that the non-guided pin and the slot are in contact at all times. Further details of the single linear pneumatic actuator are shown in Figure 3b. The single linear pneumatic actuator is mounted facing the fingers to move one or all fingers together. A telescopic shaft drives the neutral pin along the slot. This configuration is an improvement over the belt drive, as it is smaller, lighter, and features simpler construction with fewer components.

6.3 THUMB MOVEMENT USING A PNEUMATIC MOTOR

The thumb is moved in the frontal plane (Figure 16) rather than the sagittal plane. Movement is imposed by a pneumatic motor connected directly to the telescopic shaft.

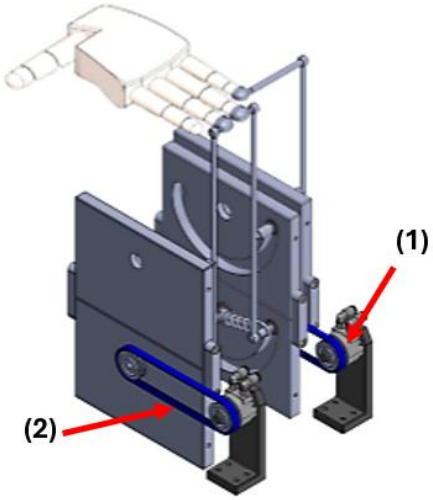

Figure 14 Finger mechanisms with belt drives.

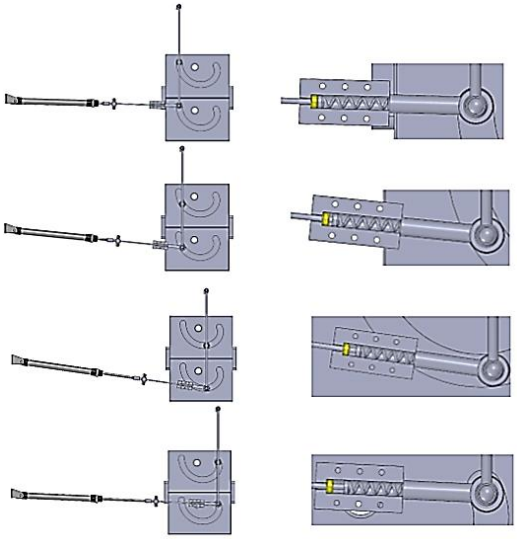

Figure 15 Fingers moved by a single pneumatic actuator.

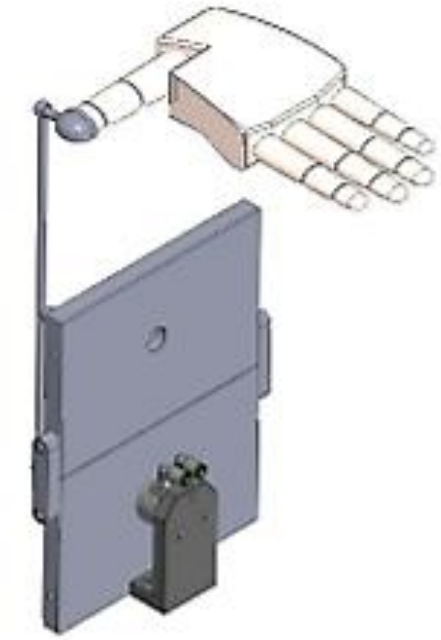

Figure 16 Pneumatic thumb motor.

7 OPERATION MODELING AND SIMULATION

Several models were constructed on a specific software platform to investigate finger movement mechanism kinematics. Simulations were carried out with various prototype geometries. In particular, the configuration where the fingers are actuated by a single linear pneumatic cylinder was analyzed. The study was carried out by operator 4. Figure 17a shows the left index finger geometry and its physiological trajectory (24 year old male subject, body mass 75 kg, height 1.85 m, proximal phalanx 45 mm, middle phalanx 30 mm, distal phalanx 20 mm). In this figure, FH is the point considered fixed on the hand, while PP, MP, DP are the extremities of each phalanx. In this finger model the geometry of each phalanx is cylindrical. Figures 17b, 17c, 17d show all the parts of the mechanism connected to this finger and moved by a single linear pneumatic actuator, analyzing its function in a succession of frames. Simulations were also carried out on the geometries for the configuration which maintains the link in the vertical position. All simulations results are good, demonstrating the study's reliability and the mechanism's ability to replicate the desired trajectory for each finger. In particular in the Figures 17b (1) is the index finger during the flexion, (2) is the vertical link, (3) is the first slot, (4) is the second slot, (5) are the trajectories of each finger phalanx, (6) are the trajectories of the slots, (7) is the telescopic shaft. During this simulation, the slots were simulated using the proper trajectories pathways. The Figure 17c shows the simulation using the cart type constraint in order to guarantee the exact vertical position of the link. Figure 18 shows the simulated trajectory of the index finger driven by the mechanism, compared with the other trajectories. A direct comparison of this trajectory

with the trajectory obtained with the same software by operator 3 (23 year old male subject, body mass 64 kg, height 179.5 cm, right index finger having 44 mm proximal phalanx, 25 mm middle phalanx, 15.5 mm distal phalanx) shows several similarities.

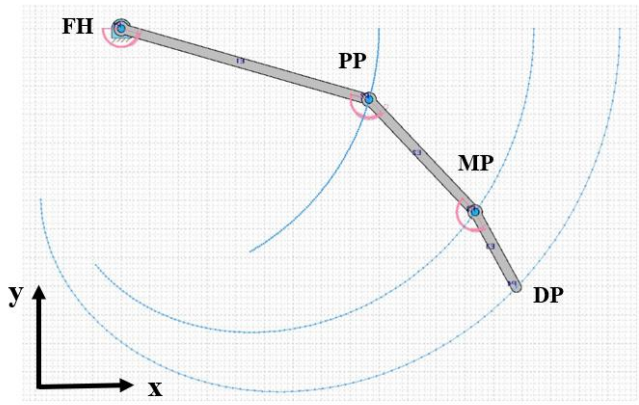

Figure 17a The index finger phalanges trajectories simulated in a specific software.

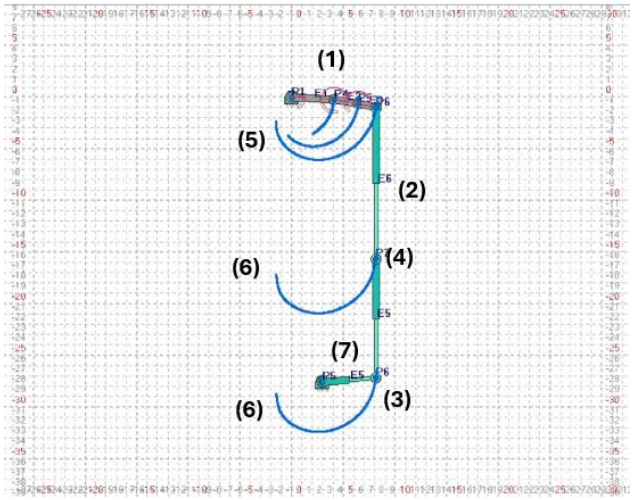

Figure 17b The index finger and its mechanism using two slots.

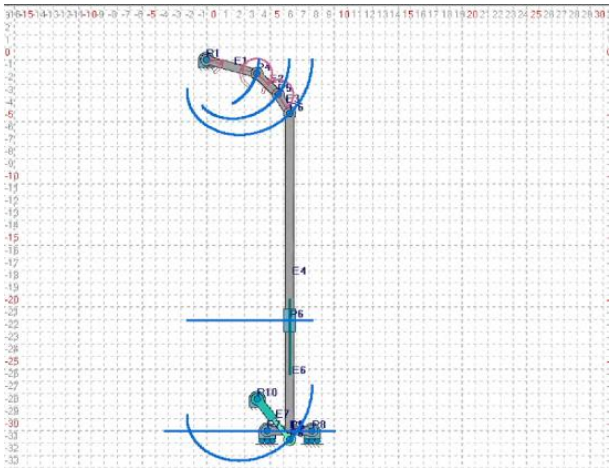

Figure 17c A simulation using the cart type constraint.

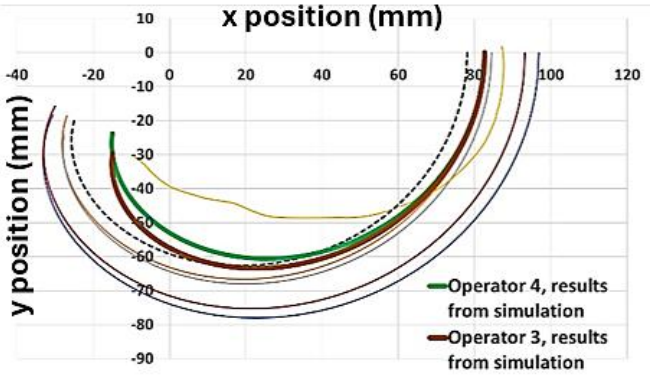

Figure 18 Comparison of simulation results and the other index finger trajectories.

The simulated trajectories show less extension than the trajectories obtained from calculations and from the experimental videos.

In fact, the simulation was influenced by the cylindrical shape of each phalanx (Figures 19a and 19b) [57], which can generate interference between the various parts of the phalanges in the finger model. It is also necessary to remember that the physiological shape of the fingers is not exactly a cylindrical one. Additional studies carried out moving the index finger (average male hand from operator 1 measurements, Table IV) manually in a CAD environment show that an imperfectly cylindrical shape (Figure 19c and 19d) of each phalanx can improve its movement and yields trajectories that are more similar to those produced from numerical considerations. With cylindrical phalanges, finger flexion (as shown by the length illustrated in the Figure 19b) is slightly less than in the case where each phalanx is modeled with a shape that is not perfectly cylindrical (Figures 19c and 19d). Further possible shapes, such as an equivalent trapezoidal shape (Figures 19e and 19f), can be analyzed to improve the finger model to avoid interference between the phalanges and to simulate full, correct finger flexion (Figure 19f). Each phalanx dimensions are here the same as those illustrated in Figures 19 a, b, c, d.

This is important in order to ensure that simulation yields realistic finger movements and trajectories in conformity with other numerical and experimental studies that can be used to investigate the articulated mechanism's kinematics.

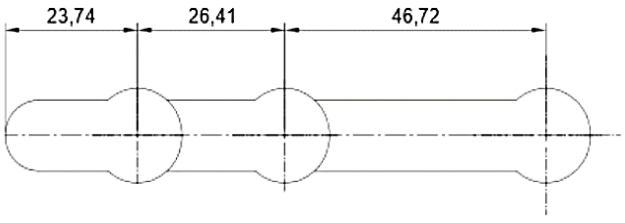

Figure 19a A CAD model of the extended index finger constructed using a cylindrical shape for each phalanx (dimensions in mm).

ISSN 1590-8844
International Journal of Mechanics and Control, Vol. 26, No. 01, 2025
https://doi.org/10.69076/jomac.2025.0009

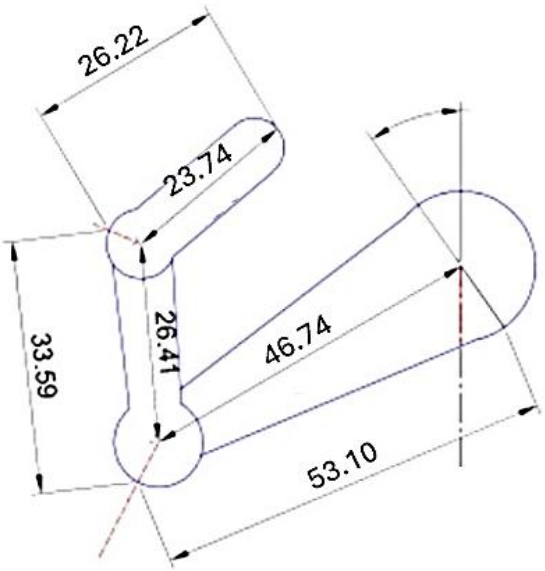

Figure 19b A CAD model of the flexed index finger constructed using a cylindrical shape for each phalanx.

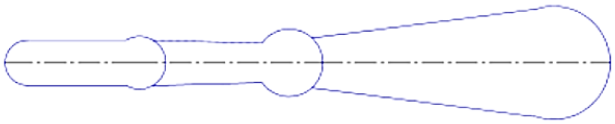

Figure 19c A CAD model of the extended index finger constructed using an imperfectly cylindrical shape for each phalanx.

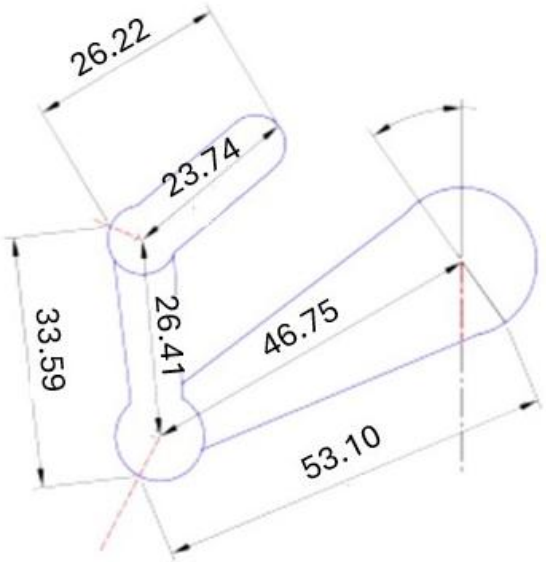

Figure 19d A CAD model of the flexed index finger constructed using an imperfectly cylindrical shape for each phalanx.

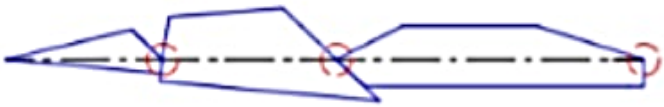

Figure 19e A further possible CAD model of the extended index finger constructed using a trapezoidal shape for each phalanx.

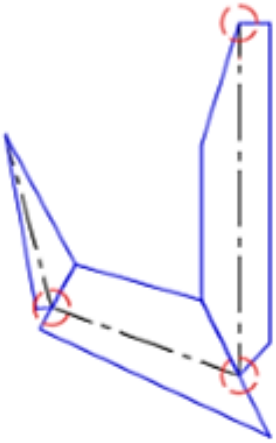

Figure 19f A further CAD model of the flexed index finger constructed using a trapezoidal shape for each phalanx.

It should be borne in mind that while the operation of the finger movement mechanism can be represented via simulation, the trajectory obtained for each finger can be influenced by the phalanx shape used in the simulation model. Assigning an appropriate geometrical shape to each phalanx during simulation is thus essential in evaluating the mechanism. The authors will address these issues in future work. The considerations presented above are useful for developing a methodology for analyzing and measuring finger trajectories, verifying the operation of the mechanism that guides them in the device presented here, and creating the slots along which each finger (or all fingers together) are guided through physiological and non-physiological motions.

8 COMPLETE PROTOTYPE: FOUR PNEUMATIC ACTUATORS

Figure 20 shows the complete prototype with its main dimensions. It has four pneumatic actuators: a pneumatic motor for thumb movement, a linear pneumatic actuator for the finger/fingers movement, a linear pneumatic actuator for the wrist movement, a linear pneumatic cylinder to move up and down all the fingers mechanisms and actuators platform. Wrist trajectories are determined using the same procedures as for the fingers. The Figure 20 shows the prototype put close to the cot in the magnetic resonance chamber. Some main dimensions of the prototype will can be improved.

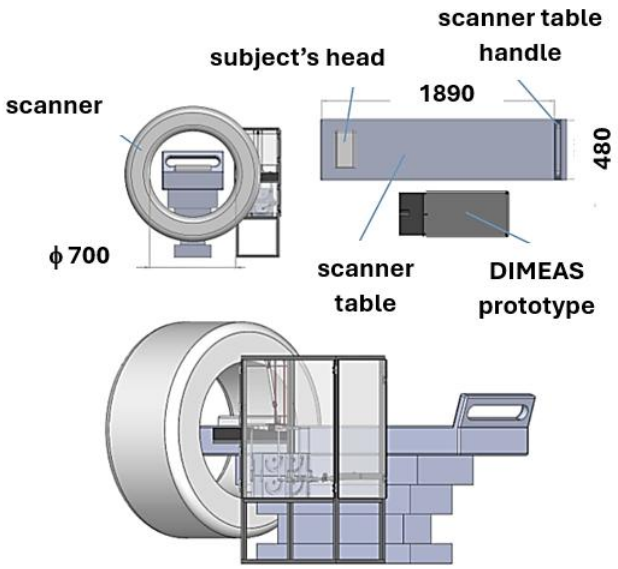

Figure 20 Some details of the prototype put inside the magnetic resonance chamber (dimensions in millimiter).

9 CONCLUSION

The paper illustrates the design process for an innovative active device capable of moving the fingers and wrist of one or both hands during fMRI analysis. The device can be used with healthy subjects and with patients. The whole structure of the machine will be improved using the movable platform to reduce the link length and removing the second slot. This is possible because the motion will never be imposed simultaneously on the wrist and fingers. For a correct use of the machine in the magnetic resonance chamber, a further check of all the materials constituting the various parts of the machine will be necessary. In any case any electronic/electrical device must be positioned outside the magnetic resonance chamber, including the electro-pneumatic control circuit. In future work, the authors plan to construct a model of the device's electropneumatic control system in order to analyze signal transaction times along 10 m long lines. The electropneumatic control system will be placed outside the magnetic resonance chamber, but the system must be able to function with the time cycle established by the clinicians. Supply pressure can be varied to impose different movement conditions on the fingers and hand, as well as to measure the subject's performance with varying levels of assistance from the device. Future construction of this device will start from development and testing of its main parts, i.e., the slots and finger movement mechanisms.The use of non-magnetic materials will necessarily lead to building many parts of the machine in plastic materials. This aspect obviously facilitates the parts in relative motion, reducing friction and improving the performance and duration of the machine itself.

AKNOWLEGEMENTS

The author thanks Prof. Katiuscia Sacco (Dept. of Psychology, University of Torino, Italy), engineers N. Ferrero, C. Gili, P. Ferrando, M. Tonaj, E. Castellaneta, M. Caddeo, and students G. Mano and A.G. Barone for their help in this study.

REFERENCES

[1] Thulborn K.R., Correlating BOLD functional magnetic resonance imaging with metabolic changes during neuronal activation should benefit the study of cognitive processing. *Nature Medicine*, Vol. 4, pp. 159-167, 1998.

[2] Ogawa S., Lee T.M., Kay A.R. and Tank D.W., Brain magnetic resonance imaging with contrast dependent on blood oxygenation. *Proc. Natl. Acad. Sci. USA*, *Biophysics*, December, Vol. 87, No. 24, pp. 9868-9872, 1990.

[3] Niola V., Penta F., Rossi C. and Savino S., An underactuated mechanical hand: Theoretical studies and prototyping. *International Journal of Mechanics and Control*, Vol. 16, No. 1, pp. 11-19, 2015.

[4] Savino S., Underactuated mechanical hand control by EMG sensors. *International Journal of Mechanics and Control*, Vol. 17, No. 1, 2016.

[5] Yap H.K., Lim J.H., Nasrallah F., Low F.Z., Goh J.C.H., Yeow R.C.H., MRC-glove: A fMRI compatible soft robotic glove for hand rehabilitation application. *2015 IEEE International Conference on Rehabilitation Robotics (ICORR)*, 11th-14th August 2015, Singapore, pp. 735-740, 2015.

[6] Yap H.K., Kamaldin N., Lim J.H., Cho Hong Goh J. and Yeow C.H., A magnetic resonance compatible soft wearable robotic glove for hand rehabilitation and brain imaging. *IEEE Transactions on Neural Systems and Rehabilitation Engineering*, Vol. 25, No. 6, pp. 782-793, 2016.

[7] Chen Y., Le S., Chu Tan Q., Lau O., Wan F. and Song C., A lobster-inspired robotic glove for hand rehabilitation. *IEEE International Conference on Robotics and Automation (ICRA)*, Singapore, 2017, pp. 4782-478, 2017.

[8] Hashida R., Matsuse H., Bekki M., Omoto M., Morimoto S., Hino T., Harano Y., Iwasa C., Miyamoto K., Haraguchi M., Nago T. and Shiba N., Evaluation of motor-assisted gloves (SEM Glove) for patients with functional finger disorders: a clinical pilot study. *Kurume Medical J.*, Vol. 65, No. 2, pp. 63-70, 2019.

[9] Chu C.Y. and Patterson R., Soft robotic devices for hand rehabilitation and assistance: a narrative review. *J. of NeuroEngineering and Rehabilitation*, Vol. 15, No. 9, pp. 1-14, 2018.

[10] Ahmed Y.S., Al-Neami A.Q. and Lateef S., Robotic glove for rehabilitation purpose: review. *Iraqi J. of*

Electrical and Electronic Eng. Conference article The 3rd Scientific Conference of Electrical and Electronic Eng., 15th-16th June 2020, Basrah Iraq, pp. 86-92, 2020.

[11] Serrano D., Copaci D., Arias J., Moreno L.E. and Blanco D., SMA-Based soft exo-glove. *IEEE Robotics and Automation Letters*, Vol. 8, No. 9, pp. 5448-5455, 2023.

[12] Liu H., Wu C., Lin S., Chen Y., Hu Y., Xu T., Yuan W. and Li Y., Finger flexion and extension driven by a single motor in robotic glove design. *Advanced Intelligent Systems*, Vol. 5, No. 5, pp. 1-10, 2023.

[13] Gorissen B., Reynaerts D., Konishi S., Yoshida K., wan Kim J. and De Volder M., Elastic inflatable actuators for soft robotic applications. *Advanced Materials*, Vol. 29, No. 43, pp. 1-14, 2017.

[14] Lambelet C., Lyu M., Wolley D., Gassert R. and Wenderoth N., The eWrist – A wearable wrist exoskeleton with sEMG-based force control for stroke rehabilitation. *Int. Conference on Rehabilitation Robotics (ICORR)*, 17th – 20th July 2017, QEII Centre, London UK, pp. 726-733, 2017.

[15] Alhamad R., Seth N. and Abdullah H.A., Initial testing of robotic exoskeleton hand device for stroke rehabilitation. *Sensors MDPI*, Vol. 23, No. 14, pp. 1-18, 2023.

[16] Jo I., Park Y., Lee J. and Bae J., A portable and spring-guided hand exoskeleton for exercising flexion/extension of the fingers. *Mechanism and Machine Theory*, Vol. 135, pp. 176-191, 2019.

[17] Aggogeri F., Mikolajczyk T. and O'Kane J., Robotics for rehabilitation of hand movement in stroke survivors. *Advances in Rehabilitation Eng. with Robotics and Mechatronics Devices*, Vol. 11, No. 4, pp. 1-14, 2019.

[18] Ratz R., Conti F., Muri R.M. and Marchal-Crespo L., A novel clinical-driven design of robotic hand rehabilitation: combining sensory training, effortless setup, and large range of motion in a palmar device. *Frontiers in Neurorobotics*, Vol. 15, pp. 1-22, 2021.

[19] Arbuckle S.A., Pruszynski J.A. and Diedrichsen J., Mapping the integration of sensory information across fingers in human sensorimotor cortex. *The Journal of Neuroscience*, Vol. 42, No. 26, pp. 5173-5185, 2022.

[20] Cobos S., Ferre M., Sanchèz Uràn M.A., Ortego J. and Pena C., Constraints for realistic hand manipulation. *10th Annual International Workshop on Presence (PRESENCE '07)*, October 2007, Barcelona Spain, pp. 369-388, 2007.

[21] Cobos S., Ferre M., Sanchèz Uràn M.A., Ortego J. and Pena C., Efficient human hand kinematics for manipulation tasks. *IEEE/RSJ International Conference on Intelligent Robots and Systems (IROS'08)*, September 2008, Nice France, pp. 2246-2251, 2008.

[22] Du Plessis T., Djouani K. and Oosthuizen C., A review of active hand exoskeletons for rehabilitation and assistance, *Robotics*, Vol. 10, No. 1, pp. 1- 42, 2021.

[23] Shimawaki, S. Nakamura Y., Nakabayashi M. and Sugimoto H., Flexion angles of finger joints in two-finger tip pinching using 3D bone models constructed from X-Ray Computed Tomography (CT) images. *Applied Bionics and Biomechanics*, pp. 1 – 6, 2020.

[24] Husaini H., Hasanuddin I., Zaqy S.Y.B. and Akhyar A., Stress analysis on mechanical hand prototype with kinematics model approach and performance tests. Disruptive Innovation in Mechanical Engineering for Industry, *Proceedings of the 3rd Int. Conference on Mechanical Eng. (ICOME 2017), published by American Institute of Physics*, 13th July 2018 Surabaya Indonesia, Vol. 1983, No. 1, pp. 1-6, 2018.

[25] Kamper D.G., Cruz E.G. and Siegel M.P., Stereotypical fingertip trajectories during grasp. *J. Neurophysiol*, Vol. 90, No. 6, pp. 3702-3710, 2003.

[26] Imbinto I., Montagnani F., Bacchereti M. and Cipriani C., The S-Finger: a synergetic externally powered digit with tactile sensing and feedback. *IEEE Transactions on Neural Systems and Rehabilitation Eng.*, Vol. 26, No. 6, pp. 1-9, 2018.

[27] Milliken G.W., Plantz E.J. and Nudo R.J., Distal forelimb representations in primary motor cortex are redistributed after forelimb restriction: a longitudinal study in adult squirrel monkeys. *J. Neurophysiol*., Vol. 109, No. 5, pp. 1268-1282, 2013.

[28] Hussain I., Santarnecchi E., Leo A., Ricciardi E., Rossi S. and Prattichizzo D., A magnetic compatible supernumerary robotic finger for functional magnetic resonance imaging (fMRI) acquisitions: device description and preliminary results. *International Conference on Rehabilitation Robotics (ICORR)*, 17th – 20th July 2017, QEII Centre, London UK, pp. 1177-1182, 2017.

[29] Carey J.R., Kimberley T.J., Lewis S.M., Auerbach E.J., Dorsey L., Rundquist P. and Ugurbil K., Analysis of fMRI and finger tracking training in subjects with chronic stroke. *Brain*, Vol. 125, pp. 773-788, 2002.

[30] De Luca C., Comani S., Di Donato L., Caulo M., Bertollo M. and Romani G.L., A-Magnetic Optic-Mechanical Device to Quantify Finger Kinematics for fMRI Studies of Bimanual Coordination. *Brain Topogr*, Vol. 19, No. 3, pp. 155–160, 2007.

[31] Lolli V., Rovai A., Trotta N., Bourguignon M., Goldman S., Sadeghi N., Jousmäki V and De Tiège X., MRI-compatible pneumatic stimulator for sensorimotor mapping. *J. of Neuroscience Methods*, Vol. 313, pp. 29-36, 2019.

[32] Pinter D., Pegritz S., Pargfrieder C., Reiter G., Wurm W., Gattringer T., Linderl-Madrutter R., Neuper C., Fazekas F., Grieshofer P. and Enzinger C., Exploratory Study on the Effects of a Robotic Hand Rehabilitation Device on Changes in Grip Strength and Brain Activity after Stroke. *Top Stroke Rehabil*, Vol. 20, No. 4, pp. 308-316, 2013.

[33] Schaechter J.D., Stokes C., Connell B.D., Perdue K and Bonmassar G., Finger motion sensors for fMRI motor studies. *NeuroImage*, Vol. 31, pp. 1549-1559, 2006.

[34] Menon S., Brantner G., Aholt C., Kay K. and Khatib O., Haptic fMRI: combining functional neuroimaging with haptics for studying the brain's motor control representation. *35th Annu Int. Conf. IEEE Eng. Med. Biol. Soc (EMBC)*, 3rd – 7th July 2013 Osaka Japan, pp. 4137-4142, 2013.

[35] Pawel L.M., *Designing of a hand rehabilitation robotic device for the post-stroke patients with flaccidity*. School of Industrial and Information Eng. Master of Science in Biomedical Eng. Master Thesis Politecnico di Milano Italy, supervisor Prof. Carlo Albino Frigo, 2019.

[36] Espinosa-Garcia F.J., Tapia-Herrera R., Lugo-Gonzalez E. and Aria-Montiel M., Design and simulation of a robotic hand with foldable palm based on mechanisms with variable topologies. *Memorias del XXI Congreso Mexicano de Robotica (XXI COMRob 2019)*, 13th-15th November 2019, Manzanito Colima Mexico, 13-15 de November, pp. 300-305, 2019.

[37] Byoung-Ho K., Analysis of coordinated motions of humanoid robot fingers using interphalangeal joint coordination. *Int. J. of Advanced Robotic Systems*, Vol. 11. No. 4, pp. 1-8, 2014.

[38] Tang Z., Sugano S. and Iwata H., A finger exoskeleton for rehabilitation and brain image study. *IEEE 13th Int. Conference on Rehabilitation Robotics*, 24th -26th June 2013 Seattle Washington USA, pp. 1-6, 2013.

[39] Carbone G., Gerding E-C., Corves B., Cafolla D., Russo M. and Ceccarelli, M., Design of a two-DOFs driving mechanism for a motion-assisted finger exoskeleton. *Applied Sciences MDPI*, Vol. 10, No. 7, pp. 1-23, 2020.

[40] Parida P.K. and Biswai B.B., Design and Analysis of a Multifingered Robot Hand. *International Journal of Robotics and Automation (IJRA)*, Vol. 1, No. 2, pp. 69-77, 2012.

[41] Liu C., Lu J., Yang H. and Guo K., Current State of Robotics in Hand Rehabilitation after Stroke: A Systematic Review. *Applied Sciences MDPI*, Vol. 12, No. 9, pp. 1-26, 2022.

[42] Vanoglio F., Bernocchi P., Mule' C., Garofali F., Mora C., Taveggia G., Scalvini S. and Luisa A., Feasibility and efficacy of a robotic device for hand rehabilitation in hemiplegic stroke patients: a randomized pilot controlled study. *Clinical Rehabilitation*, Vol. 31, No. 3, pp. 351-360, 2017.

[43] Sacco K., *Neuroimaging per lo studio del cervello umano*. II edition, Idelson Gnocchi Ed., 5th June 2020, pp. 1-260, 2020.

[44] Belforte G., Eula G., Sirolli S., Bois P., Geda E., D'Agata F., Cauda F., Duca S., Zettin M., Virgilio R., Geminiani G. and Sacco K., Bra.Di.P.O. and P.I.G.R.O.: Innovative devices for motor learning programs. *Journal of Robotics*, Vol. 2014, pp. 1-12, 2014.

[45] Agrawal J., Raichandani L., Sushma K. and Surbhi Raichandani S., Estimation of stature from hand length and length of phalanges. *Journal of Evolution of Medical and Dental Sciences*, Vol. 2, No. 50, pp. 9651-9656, 2013.

[46] Bures M., Gorner T. and Sediva B., Hand anthropometry of Czech population. *2015 IEEE Int. Conference on Industrial Eng. and Eng. Management* (IEEM), Singapore pp. 1-7, 2015.

[47] Guerra R.S., Fonseca I., Pichel F., Restivo M.T. and Amaral T.F., Hand length as an alternative measurement of height. *Eur J Clin Nutr*, Vol. 68, No. 2, pp. 229-233, 2014.

[48] Kondo M., Ogihara N., Shinoda K., Anada S., Ito K., Murata M., Tanaka T., Takai S. and Matsu'ura S., Sexual dimorphism in the human hand proportion: A radiographic study. *Bull. Natl. Mus. Nat. Sci*, Vol. 43, pp. 1-6, 2017.

[49] Buryanov A. and Kotuk V., Proportions of hand segments. *Int. J. Morphol*, Vol. 28, No. 3, pp. 755-758, 2010.

[50] Herman I.P., *Physics of the Human Body*. 2nd Edition, Springer Verlag, 2016.

[51] Penn State Eberly College of Science, 2.6 – (Pearson) Correlation coefficient r. *STAT 462 lesson Applied Regression Analysis*, Dept. of Statistics Online Programs, 2018.

[52] Anderson T.W. and Darling D.A., Asymptotic theory of certain "goodness-of-fit" criteria based on stochastic processes. *Annals of Mathematical Statistics*, Vol. 23, No. 2, pp. 193–212. 1952.

[53] Shapiro S.S. and Wilk M.B., An analysis of variance test for normality (complete samples). *Biometrika*, Vol. 52, No. 3 and 4, pp. 591-611, 1965.

[54] Blair R.C. and Higgins J.J., A Comparison of the Power of Wilcoxon's Rank-Sum Statistic to That of Student's t Statistic under Various Nonnormal Distributions. *Journal of Educational Statistics*, Vol. 5, No. 4 pp. 309-335, 1980.

[55] Conley T. and Taber C. Inference with "Difference in Differences" with a Small Number of Policy Changes. *NBER Technical Working Paper*, No. 312, pp. 1-51, 2005.

[56] Lane D., *Difference between two means*. LibreTexts Statistics Libraries, 2022.

[57] Lin J., Wu Y. and Huang T.S., Modeling the constraints of human hand motion. *Prodeedings Workshop on Human Motion*, 7th-8th December 2000, Austin Texas USA, pp. 121-126, 2000.